THE JOURNAL OF PHYSICAL CHEMISTRY Letters

Letter

pubs.acs.org/JPCL

Mid-Infrared Time-Resolved Frequency Comb Spectroscopy of Transient Free Radicals

Adam J. Fleisher,*[,†,‡] Bryce J. Bjork,[†] Thinh Q. Bui,[§] Kevin C. Cossel,[†] Mitchio Okumura,*[,§] and Jun Ye*[,†]

[†]JILA, National Institute of Standards and Technology and University of Colorado, Department of Physics, 440 UCB, Boulder, Colorado 80309, United States

[‡]Material Measurement Laboratory, National Institute of Standards and Technology, 100 Bureau Drive, Gaithersburg, Maryland 20899, United States

[§]Arthur Amos Noyes Laboratory of Chemical Physics, Division of Chemistry and Chemical Engineering, California Institute of Technology, 1200 East California Boulevard, Pasadena, California 91125, United States

Supporting Information

ABSTRACT: We demonstrate time-resolved frequency comb spectroscopy (TRFCS), a new broadband absorption spectroscopy technique for the study of trace free radicals on the microsecond timescale. We apply TRFCS to study the time-resolved, mid-infrared absorption of the deuterated hydroxyformyl radical *trans*-DOCO, an important short-lived intermediate along the OD + CO reaction path. Directly after photolysis of the chemical precursor acrylic acid-d_1, we measure absolute *trans*-DOCO product concentrations with a sensitivity of 5×10^{10} cm^{-3} and observe its subsequent loss with a time resolution of 25 μs. The multiplexed nature of TRFCS allows us to detect simultaneously the time-dependent concentration of several other photoproducts and thus unravel primary and secondary chemical reaction pathways.

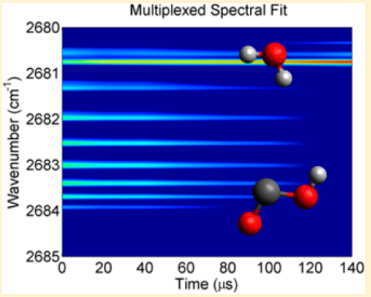

SECTION: Spectroscopy, Photochemistry, and Excited States

Norrish and Porter's seminal work on flash photolysis heralded the beginning of quantitative studies in gas-phase free-radical chemistry.[1] There have been remarkable experimental advances since then in the time-resolved detection of transient free radicals to directly measure product spectra, concentrations, branching ratios, or reaction rate coefficients. However, acquiring truly multiplexed spectral data regarding several species in a fast chemical reaction with high-frequency resolution and fast time resolution over a broad spectral bandwidth remains a technical challenge. Ultrasensitive single-species detection limits can be achieved using continuous-wave (cw) laser absorption techniques with narrow single wavelength detection, but this approach requires relatively slow scans to cover wide spectral ranges. Traditional multiplexed techniques such as time-resolved mid-infrared (mid-IR) spectroscopy use a step-scan Fourier transform approach, and newer cavity-enhanced methods using light-emitting diodes provide the desired microsecond (or better) time resolution and broad bandwidth but normally with an incoherent light source and thus long total acquisition times to achieve high sensitivity.[2,3] Techniques that improve upon these state-of-the-art methods would have wide-ranging applications such as direct measurements of carbonyl oxides formed during the ozonolysis of alkenes,[4−7] understanding unexplained OH radical concentrations in the atmosphere,[8,9] and verification of nuclear-spin selection rules in reactions of polyatomics.[10]

Mid-IR frequency combs generated using coherent, high-powered femtosecond fiber lasers have recently been developed that unify these three desired traits: high detection sensitivity, large spectral bandwidth, and fast time resolution.[11] The advent of the phase-stabilized femtosecond optical frequency comb merged the seemingly divergent fields of ultrafast spectroscopy performed with temporally short laser pulses and the ultraprecise measurement of optical frequencies using stable cw lasers.[12] The optical frequency comb has proven to be an invaluable tool for the transfer of precise microwave frequency standards into the optical domain, allowing for the direct interrogation of atomic eigenstates with unprecedented precision while also probing time-dependent quantum coherence effects.[13] Because of their broad spectral bandwidth but inherently high resolution, frequency combs have found applications as sources for trace-gas detection and broadband survey spectroscopy.[11,14−17] Here we make use of these remarkable advances in optical physics and laser stabilization to address current problems in free-radical trace detection and chemical kinetics. Our technique, named time-resolved frequency comb spectroscopy (TRFCS), enables transient molecular absorption spectroscopy on the microsecond time scale with rovibrational state resolution (0.03 cm^{-1}) simulta-

Received: April 30, 2014
Accepted: June 10, 2014
Published: June 10, 2014

   dx.doi.org/10.1021/jz5008559 | J. Phys. Chem. Lett. 2014, 5, 2241−2246

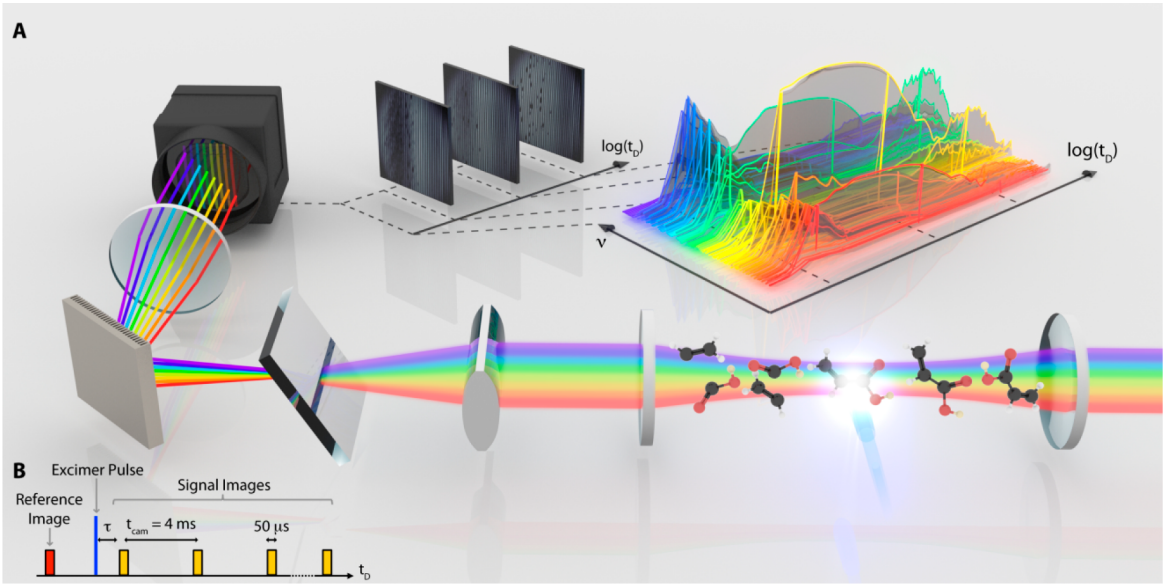

Figure 1. (A) Illustration of time-resolved frequency comb spectroscopy (TRFCS) performed with a high-finesse optical cavity coupled to a reaction flow cell. The time delay between photolysis and spectral acquisition provides microsecond time resolution over a broad spectral bandwidth of 65 cm^{-1} in the mid-infrared (mid-IR). (B) Block diagram of the data acquisition scheme, where time zero (t_D = 0 μs) is defined by the photolysis pulse (blue).

neously over a 65 cm^{-1} spectral bandwidth. TRFCS, demonstrated here in the important mid-IR spectral region, allows for the reactivity of several species to be observed in a single spectrum with noise-equivalent absorption (NEA) sensitivity of 1×10^{-9} cm^{-1} $Hz^{-1/2}$ per spectral element. The ability to measure multiple species simultaneously can then rapidly provide precise rate coefficients and branching ratios for multiple reactions.

For this initial demonstration of TRFCS, we studied the time-resolved absorption of a deuterated analogue of the HOCO radical, an important short-lived intermediate in the OH + CO → H + CO_2 reaction. Throughout Earth's lower atmosphere, this reaction recycles hydroxyl (OH) radical to hydroperoxy (HO_2) radical and is important in radical reaction cycles that determine ozone concentrations.[18] This reaction also serves as the primary oxidation pathway for carbon monoxide (CO) to form carbon dioxide (CO_2), therefore regulating the global concentrations of both species.[19] In addition, OH + CO → H + CO_2 is critical in the combustion of fossil fuels, where it is also the primary route for converting CO to CO_2 and accounts for a major fraction of the heat released.[20] The kinetics of OH + CO is complicated by an anomalous temperature dependence; near room temperature, the reaction rate coefficient deviates significantly from a simple Arrhenius expression due to formation of the HOCO intermediate. Two structures have been identified, the *cis* and *trans* conformers of HOCO,[21,22] with the *trans*-HOCO conformer more stable by ~7 kJ mol^{-1}.[23,24] Although this reaction has been studied extensively, quantitative yields of HOCO would provide a direct test of statistical rate models and tunneling effects.[25]

As a first step toward this goal, we demonstrate the applicability of TRFCS for detecting trace transient HOCO intermediates by measuring the absolute concentration and subsequent reaction rate of deuterated *trans*-HOCO (*trans*-DOCO) following laser photolysis of acrylic acid-d_1 ($H_2CCHCOOD$, AA-d_1, 90% isotopic purity) via detection of the *trans*-DOCO OD fundamental stretch.[26] The photodissociation of AA/AA-d_1, an α-unsaturated acid, is a well-known source of HOCO/DOCO. The broadband capability of TRFCS allows us not only to detect the prompt *trans*-DOCO products but also to observe the depletion of parent AA-d_1 and to observe other primary and secondary photochemical products.

An illustration of the experimental apparatus is shown in Figure 1A. A mid-IR frequency comb with its output spectrum centered at 2680 cm^{-1} (3.73 μm) was coupled to a high-finesse enhancement cavity (finesse of 1250) that also functioned as a reaction flow cell for photolysis experiments.[27,28] In the frequency domain, the frequency comb teeth correspond to unique frequencies $f_m = mf_{rep} + f_{ceo}$, where m is the comb tooth index (on the order of 10^5), f_{rep} is the repetition rate of the mode-locked laser, and f_{ceo} corresponds to the carrier-envelope offset within the individual ultrashort laser pulses.[12] By dithering the femtosecond pump laser cavity length, we dither f_{rep} at a rate of 50 kHz, causing the individual frequency comb teeth to be swept through their respective enhancement cavity modes (separated by the free spectral range (FSR) of the external cavity). This results in a large peak in cavity transmission because many frequency comb modes are simultaneously resonant with the cavity. A small portion of the total power contained in these large cavity transmission peaks was used to generate a feedback signal for fast f_{ceo} stabilization (via the OPO cavity length) and slow enhancement cavity length stabilization (via a PZT mounted on the second enhancement cavity mirror), thus ensuring maximum cavity-comb coupling at the center of each dither half-period.[15] The majority of the broadband frequency comb light transmitted through the cavity (~150 cm^{-1} bandwidth) was spatially dispersed using a cross-dispersed virtually imaged phased array (VIPA) spectrometer with 1 GHz (0.03 cm^{-1}) resolution,[29] which set the resolution of the spectra measured here. This spectrometer mapped individual optical frequencies to points on an image plane, allowing for the simultaneous multiplexed detection of differential cavity transmission on time

dx.doi.org/10.1021/jz5008559 | J. Phys. Chem. Lett. 2014, 5, 2241−2246

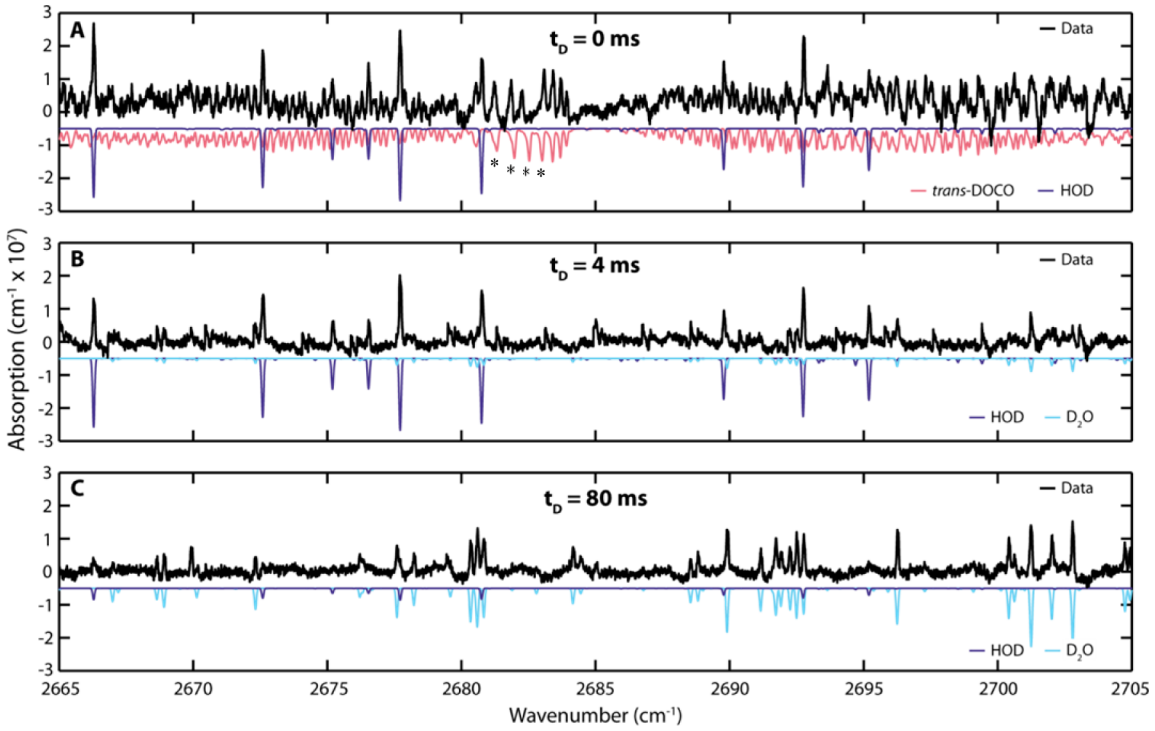

Figure 2. Transient absorption following the photolysis of acrylic acid-d_1 (AA-d_1). (A) Experimental spectrum recorded immediately following photolysis (t_D = 0 μs) is shown in black, along with fitted simulations of *trans*-DOCO (red) and HOD (dark blue) spectra, which are inverted and offset (by 0.5 × 10^{-7} cm^{-1}) for clarity. The four transitions marked with an asterisk (*) are known to be perturbed by a Coriolis or Fermi interaction[26] and therefore were not included in any fits of *trans*-DOCO concentration. (B) Experimental trace at t_D = 4 ms, where the concentration of *trans*-DOCO has decayed below our detection limits. Spectral fits at t_D = 4 ms (HOD in dark blue, D_2O in light blue) are again inverted and offset. (C) Experimental trace at t_D = 80 ms with inverted and offset spectral fits (HOD in dark blue, D_2O in light blue).

scales limited ultimately by molecular decoherence.[13] The size of the detector array limited our instantaneous spectral bandwidth to 65 cm^{-1}, which was resolved into 1930 elements (7072 comb teeth). A mixture of AA-d_1, CO_2, and N_2 (1.60 kPa total pressure and 21 °C) flowed continuously through the central 12 cm of the cavity, refreshing gas in the photolysis region on a <1 s time scale. High flows of purge gas were introduced to keep the mirrors clean. Typical final concentrations of AA-d_1 in the cell were on the order of 4 × 10^{14} cm^{-3}. A 10 ns, 193 nm laser pulse from an ArF excimer laser (~5 mJ per pulse within a 3 cm × 1 cm photolysis region) was used to initiate photolysis[30] and defined time zero (t_D = 0 μs) for subsequent DOCO kinetics. Images from the VIPA spectrometer were recorded before and after the excimer pulse with integration times of either 25 or 50 μs. The excimer laser repetition rate was 0.2 Hz, allowing for the high-finesse flow cell to be replenished with fresh AA-d_1 sample before each subsequent photolysis experiment.

In a typical experimental cycle, a sequence of 200 transient absorption spectra was recorded, each delayed by a total time relative to the single 193 nm photolysis pulse of $t_D = (n-1)t_{cam} + \tau$, where n is the signal image number (1 to 200), t_{cam} is the constant delay between successive camera images (4 ms) limited by the camera frame rate, and τ is a variable μs time delay. (See Figure 1B.) Several sections of the 1-D absorption spectra constructed from these images[31] are shown in Figure 2. Each spectrum is the average over 950 cycles with an integration time of 50 μs for individual camera images. Slow baseline fluctuations, periodic oscillations, and the AA-d_1 photodepletion spectrum have been subtracted from the experimental traces. Figure 2A shows the experimental spectrum recorded at a time delay of t_D = 0 μs, that is, within the first 50 μs after photolysis. Simulations of the individual molecular contributions to the spectral fit are shown, inverted and offset for clarity.

At t_D = 0 μs, rovibrational features of *trans*-DOCO could be unambiguously assigned using previously determined spectroscopic parameters and calculated intensities.[26,32,33] By fitting the observed spectral features to the simulated spectrum, we measured the absolute molecular concentration of *trans*-DOCO within this 50 μs integration window to be 3.1 × 10^{12} cm^{-3} ± 0.5 × 10^{12} cm^{-3} (1σ total experimental uncertainty; see Supporting Information). The statistical uncertainty in the spectral fit of *trans*-DOCO molecules was 5 × 10^{10} cm^{-3}, a direct result of the multiline fitting routines possible when performing broadband spectroscopy.[27] We also observed a prompt (within 50 μs) formation of HOD within this spectral window. At t_D = 4 ms (Figure 2B), the absolute concentration of *trans*-DOCO had dropped below our detection limit, leaving only strong absorption features from HOD, along with new, weaker features from D_2O arising from isotopic exchange reactions with AA-d_1. At a longer time delay of t_D = 80 ms (Figure 2C), the HOD had mostly decayed, and strong absorptions from D_2O dominated the spectral window, indicating that the flow system has been fully passivated with deuterium and that there is little or no contamination by H_2O.

To investigate the submillisecond decay of *trans*-DOCO, we obtained a set of interleaved time-series spectra by stepping the time delay τ in 20 μs increments. These spectra were recorded with a camera-limited integration time of 25 μs, beginning 40 μs before the photolysis pulse (t_D = −40 μs). In total, we use 13 different values of τ over the range −40 μs ≤ τ ≤ 200 μs,

dx.doi.org/10.1021/jz5008559 | J. Phys. Chem. Lett. 2014, 5, 2241−2246

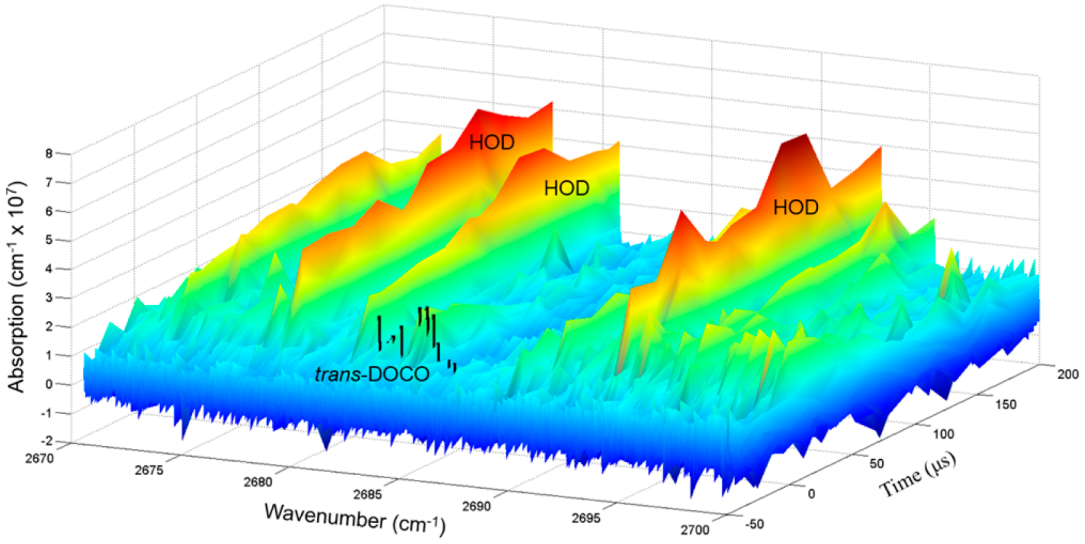

Figure 3. *trans*-DOCO absorption and decay measured in the first 200 μs following photolysis of AA-d_1. The strong *trans*-DOCO *Q*-branch lines are outlined in black. Increasing absorption from HOD product is also visible.

acquiring 200 spectra at the camera frame rate at each unique value of τ. These interleaved time-series spectra were averaged 50 times and are shown for $t_D \leq 200$ μs in Figure 3 as a 3-D surface. The strongest *trans*-DOCO *Q*-branch transitions, ~2684 cm^{-1}, are outlined in black; they decayed much faster than the overall rise in surrounding HOD absorption. From spectral fits to the data shown in Figures 2 and 3 as well as that shown in the Supporting Information,[33] we obtained time-dependent absolute concentrations of *trans*-DOCO, HOD, and D_2O (Figure 4). In addition to these three species, we also detected (in a different spectral region) the immediate formation of C_2HD following photolysis;[33] its time-dependent concentration is plotted in Figure 4. Within the time integration window immediately after excimer photolysis, HOD, C_2HD, and *trans*-DOCO were all formed instantaneously after the first photolysis laser shot and after all subsequent duty cycles (Figure 4B,C).

Immediately after photolysis, within the first 25 μs for *trans*-DOCO and HOD and the first 50 μs for C_2HD, we measure concentrations of 6.0×10^{12} cm^{-3} $\pm$ 0.5×10^{12} cm^{-3}, 1.20×10^{13} cm^{-3} $\pm$ 0.07×10^{13} cm^{-3}, and 7×10^{11} cm^{-3} $\pm$ 3×10^{11} cm^{-3}, respectively. Of these products, only *trans*-DOCO has been reported previously.[30] At our low partial pressures of AA-d_1 (~1 Pa), no secondary reactions were possible within the first 50 μs, diffusion to/from walls is too slow, and we therefore deduce that these products were not formed by subsequent radical chemistry.

Over the subsequent 200 μs after photolysis, we observed a rapid decay in *trans*-DOCO and a slight rise in the concentration of HOD on time scales consistent with bimolecular reactions. The effective first-order rate coefficient, $k'_{tDOCO,\,eff} = 9.6 \times 10^3$ s^{-1} $\pm$ 0.9×10^3 s^{-1}, is similar to HOCO loss rates observed by Petty, Harrison, and Moore under similar conditions, which they attribute to fast bimolecular reactions with radical intermediates,[34] for example, the vinyl radical or DOCO. At longer times (>200 μs), D_2O grows in as HOD decays, likely due to isotope exchange reactions HOD + HOD and HOD + AA-d_1. While OH products have been observed by laser-induced fluorescence, the yield has not been measured.[35,36] Our detection limit for OD absorption within our probe wavelength range is ~5×10^{12} cm^{-3}, and we find no evidence of OD production above this minimum detectable level.[33] This observation is consistent with those of Osborne, Li, and Smith, who have reported that CO (and implicitly OH) is formed in nearly equal concentrations with HOCO following AA photolysis under similar experimental conditions.[37]

Our observation of prompt HOD and C_2HD products is unexpected, and we speculate that these may be formed from the unimolecular decomposition of AA-d_1, which possess 620 kJ mol^{-1} of internal energy. These could be coproducts from the previously observed decarboxylation or decarbonylation channels,[37] resulting from hydrogen migration or abstraction pathways[38] similar to mechanisms seen in the 193 nm photolysis of propene.[39] In molecular beam experiments, Kitchen et al. find that 193 nm photodissociation leads to only two prompt channels, C−C bond fission (HOCO + C_2H_3) and C−O bond fission (OH + C_2H_3CO) under collisionless conditions,[30] although in the bulk gas, other products could be formed by collisional dissociation of vibrationally hot intermediates or relaxation to long-lived, electronically excited AA* with alternate unimolecular pathways. However, acrylic acid forms strong hydrogen bonds and is known to be "sticky", and our current experiments do not allow us to definitively eliminate alternative explanations (artifacts such as wall contamination or photochemistry, H_2O impurities, photolysis of AA-dimers or AA-water clusters). Further experiments are needed to test the validity of the above hypothesis.[33]

Our results on acrylic acid photodissociation highlight how the high molecular sensitivity (10^{10} cm^{-3}) and broad spectral coverage (65 cm^{-1}) of mid-IR time-resolved frequency comb spectroscopy enable the identification and characterization of multiple transient species simultaneously (including, under more carefully controlled experimental conditions, their respective photolysis yields and branching ratios), while the high time resolution can give precise information about the subsequent reaction rates. The coherent nature of TRFCS provides its high sensitivity, as laser phase stabilization results in the concentration of optical power into narrow, discrete frequencies (that is, comb teeth). In this initial implementation, we demonstrate sensitive detection of *trans*-DOCO in the mid-IR toward the study of DOCO produced in the OD + CO

dx.doi.org/10.1021/jz5008559 | *J. Phys. Chem. Lett.* 2014, 5, 2241−2246

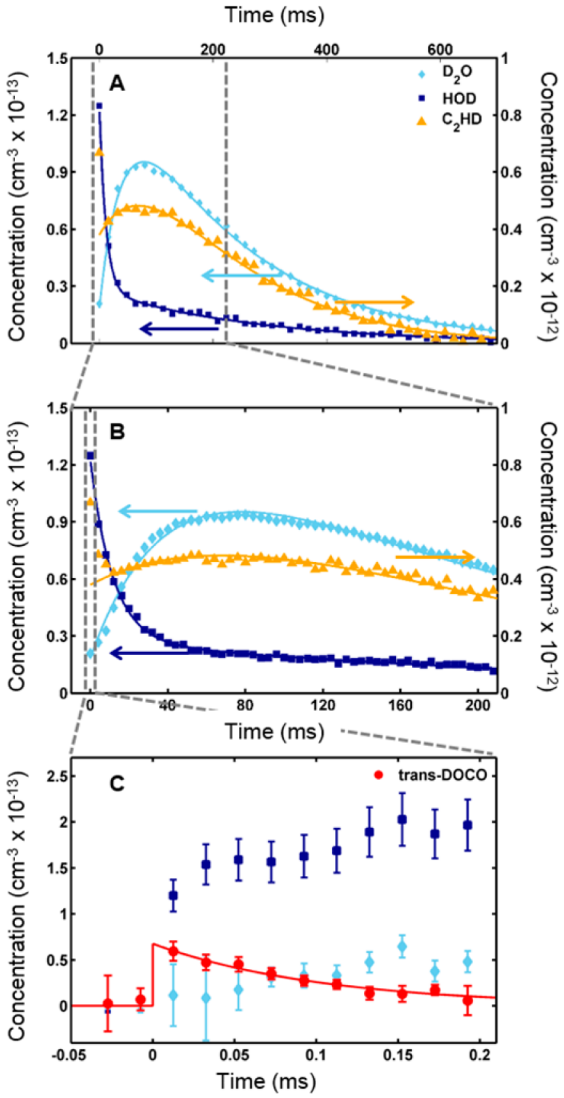

Figure 4. (A) Measured absolute concentrations of HOD (dark-blue squares), D_2O (light-blue diamonds), and C_2HD (orange triangles) with a 50 μs integration time and ~0.05 s of averaging. For clarity, only every fourth data point is shown. Empirical fits to biexponential functions are plotted as solid lines of the appropriate color for each observed molecular signal. The data plotted here are influenced by two types of instrument response: diffusion of primary photoproducts out of the comb probe beam on short time scales and net flow out of the cell due to continuous pumping on longer times. (B) Zoom from 0 to 200 ms of the data in panel A, now showing all data points. In both panels A and B, the concentration axis for HOD and D_2O is on the left, whereas the concentration of C_2HD (smaller in scale by an order of magnitude) is shown on the right. (C) Measured absolute concentrations of HOD, D_2O, and *trans*-DOCO (red circles) at times ≤200 μs (25 μs integration time). Experimental error bars are shown at 1σ. The decay of *trans*-DOCO was empirically fit to an effective first-order loss with a coefficient $k'_{tDOCO,eff} = 9.6 \times 10^3\ s^{-1} \pm 0.9 \times 10^3\ s^{-1}$ (solid red line).

reaction. Time-resolved spectroscopy of this and many other fast radical reactions would benefit from the unique characteristics of highly coherent ultrafast lasers, which now provide frequency combs from the mid-IR to the extreme ultraviolet.[40]

■ ASSOCIATED CONTENT

Ⓢ Supporting Information

Additional details regarding materials and methods, fitting procedures, C_2HD spectroscopy, experimental uncertainty, TRFCS performance, and flow cell residence time. This material is available free of charge via the Internet at http://pubs.acs.org.

■ AUTHOR INFORMATION

Corresponding Authors

*E-mail: adam.fleisher@nist.gov (A.J.F.).
*E-mail: mo@caltech.edu (M.O.).
*E-mail: ye@jila.colorado.edu (J.Y.).

Notes

The authors declare no competing financial interests.

■ ACKNOWLEDGMENTS

We thank Keeyoon Sung of the National Aeronautics and Space Administration (NASA) Jet Propulsion Laboratory (JPL) for providing a list of D_2O mid-IR line positions and intensities measured by Robert A. Toth of JPL. We are grateful to Scott A. Diddams of the National Institute of Standards and Technology (NIST) and Tim Dinneen of Precision Photonics for providing the mid-IR VIPA etalon used in this work. We also thank Brad Baxley for artistic contributions to Figure 1 and acknowledge financial support from NIST, NSF, NASA, AFOSR, and DTRA. Adam J. Fleisher was supported by a National Research Council postdoctoral fellowship and Thinh Bui by a NASA Earth and Space Science Fellowship.

■ REFERENCES

(1) Porter, G. In *The Chemical Bond: Structure and Dynamics*; Zewail, A. H., Ed.; Academic Press: Boston, 1992; pp 113−148.
(2) Toscano, J. P. In *Reviews of Reactive Intermediate Chemistry*; Platz, M. S., Moss, R. A., Jones, M., Jr., Eds.; Wiley: Hoboken, NJ, 2007; pp 183−205.
(3) Ball, S. M.; Povey, I. M.; Norton, E. G.; Jones, R. L. Broadband Cavity Ringdown Spectroscopy of the NO_3 Radical. *Chem. Phys. Lett.* **2001**, *342*, 113−120.
(4) Welz, O.; Savee, J. D.; Osborn, D. L.; Vasu, S. S.; Percival, C. J.; Shallcross, D. E.; Taatjes, C. A. Direct Kinetic Measurements of Criegee Intermediate (CH_2OO) Formed by Reaction of CH_2I with O_2. *Science* **2012**, *355*, 204−207.
(5) Su, Y.-T.; Huang, Y.-H.; Witek, H. A.; Lee, Y.-P. Infrared Absorption Spectrum of the Simplest Criegee Intermediate CH_2OO. *Science* **2013**, *340*, 174−176.
(6) Taatjes, C. A.; Welz, O.; Eskola, A. J.; Savee, J. D.; Scheer, A. M.; Shallcross, D. E.; Rotavera, B.; Lee, E. P. F.; Dyke, J. M.; Mok, D. K. W.; et al. Direct Measurements of Conformer-Dependent Reactivity of the Criegee Intermediate CH_3CHOO. *Science* **2013**, *340*, 177−180.
(7) Su, Y.-T.; Lin, H.-Y.; Putikam, R.; Matsui, H.; Lin, M. C.; Lee, Y.-P. Extremely Rapid Self-Reaction of the Simplest Criegee Intermediate CH_2OO and its Implications in Atmospheric Chemistry. *Nat. Chem.* **2014**, *6*, 477−483.
(8) Levieveld, J.; Butler, T. M.; Crowley, J. N.; Dillon, T. J.; Fischer, H.; Ganzeveld, L.; Harder, H.; Lawrence, M. G.; Martinez, M.; Taraborreli, D.; et al. Atmospheric Oxidation Capacity Sustained by a Tropical Forest. *Nature* **2008**, *452*, 737−740.
(9) Mauldin, R. L., III; Berndt, T.; Sipilä, M.; Paasonen, P.; Petäjä, T.; Kim, S.; Kurtén, T.; Stratmann, F.; Kerminen, V.-M.; Kulmala, M. A New Atmospherically Relevant Oxidant of Sulphur Dioxide. *Nature* **2012**, *488*, 193−197.
(10) Oka, T. Nuclear Spin Selection Rules in Chemical Reactions by Angular Momentum Algebra. *J. Mol. Spectrosc.* **2004**, *228*, 636−639.

(11) Schliesser, A.; Picqué, N.; Hänsch, T. W. Mid-Infrared Frequency Combs. *Nat. Photonics* **2012**, *6*, 440−449.
(12) Cundiff, S. T.; Ye, J. Colloquium: Femtosecond Optical Frequency Combs. *Rev. Mod. Phys.* **2003**, *75*, 325−342.
(13) Marian, A.; Stowe, M. C.; Lawall, J. R.; Felinto, D.; Ye, J. United Time-Frequency Spectroscopy for Dynamics and Global Structure. *Science* **2004**, *306*, 2063−2068.
(14) Thorpe, M. J.; Moll, K. D.; Jones, R. J.; Safdi, B.; Ye, J. Broadband Cavity Ringdown Spectroscopy for Sensitive and Rapid Molecular Detection. *Science* **2006**, *311*, 1595−1599.
(15) Adler, F.; Thorpe, M. J.; Cossel, K. C.; Ye, J. Cavity-Enhanced Direct Frequency Comb Spectroscopy: Technology and Applications. *Annu. Rev. Anal. Chem.* **2010**, *3*, 175−205.
(16) Newbury, N. R. Searching for Applications with a Fine-Tooth Comb. *Nat. Photonics* **2011**, *5*, 186−188.
(17) Gilli, R.; Méjean, G.; Kassi, S.; Ventrillard, I.; Abd-Alrahman, C.; Romanini, D. Frequency Comb Based Spectrometer for *in Situ* and Real Time Measurements of IO, BrO, NO_2, and H_2CO at pptv and ppqv Levels. *Environ. Sci. Technol.* **2012**, *46*, 10704−10710.
(18) Crutzen, P. J. In *Low-Temperature Chemistry of the Atmosphere*; Moortgat, G. K., Barnes, A. J., Le Bras, G., Sodeau, J. R., Eds.; Springer-Verlag: Berlin, 1994; pp 465−498.
(19) Wayne, R. P. *Chemistry of Atmospheres*; Oxford University Press: New York, 2000.
(20) Glassman, I.; Yetter, R. A. *Combustion*; Academic Press: New York, 2008.
(21) Francisco, J. S.; Muckermann, J. T.; Yu, H.-G. HOCO Radical Chemistry. *Acc. Chem. Res.* **2010**, *43*, 1519−1526.
(22) Oyama, T.; Funato, W.; Sumiyoshi, Y.; Endo, Y. Observation of the Pure Rotational Spectra of *trans*- and *cis*-HOCO. *J. Chem. Phys.* **2011**, *134*, 174303.
(23) Nguyen, T. L.; Xue, B. C.; Weston, R. E., Jr.; Barker, J. R.; Stanton, J. F. Reaction of HO with CO: Tunneling is Indeed Important. *J. Phys. Chem. Lett.* **2012**, *3*, 1549−1553.
(24) Weston, R. E., Jr.; Nguyen, T. L.; Stanton, J. F.; Barker, J. R. HO + CO Reaction Rates and H/D Kinetic Isotope Effects: Master Equation Models with ab initio SCTST Rate Constants. *J. Phys. Chem. A* **2013**, *117*, 821−835.
(25) Guo, H. Quantum Dynamics of Complex-Forming Bimolecular Reactions. *Int. Rev. Phys. Chem.* **2012**, *31*, 1−68.
(26) Petty, J. T.; Moore, C. B. Transient Infrared Absorption Spectrum of the ν_1 Fundamental of *trans*-DOCO. *J. Chem. Phys.* **1993**, *99*, 47−55.
(27) Adler, F.; Masłowski, P.; Foltynowicz, A.; Cossel, K. C.; Briles, T. C.; Hartl, I.; Ye, J. Mid-Infrared Fourier Transform Spectroscopy with a Broadband Frequency Comb. *Opt. Express* **2010**, *18*, 21861−21872.
(28) Mollner, A. K.; Valluvadasan, S.; Feng, L.; Sprague, M. K.; Okumura, M.; Milligan, D. B.; Bloss, W. J.; Sander, S. P.; Martien, P. T.; Harley, R. A.; et al. Rate of Gas Phase Association of Hydroxyl Radical and Nitrogen Dioxide. *Science* **2010**, *330*, 646−649.
(29) Nugent-Glandorf, L.; Neely, T.; Adler, F.; Fleisher, A. J.; Cossel, K. C.; Bjork, B. J.; Dinneen, T.; Ye, J.; Diddams, S. A. Mid-Infrared Virtually Imaged Phased Array Spectrometer for Rapid and Broadband Trace Gas Detection. *Opt. Lett.* **2012**, *37*, 3285−3287.
(30) Kitchen, D. C.; Forde, N. R.; Butler, L. J. Photodissociation of Acrylic Acid at 193 nm. *J. Phys. Chem. A* **1997**, *101*, 6603−6610.
(31) Diddams, S. A.; Hollberg, L.; Mbele, V. Molecular Fingerprinting with the Resolved Modes of a Femtosecond Laser Frequency Comb. *Nature* **2007**, *445*, 627−630.
(32) Huang, X.; Fortenberry, R. C.; Wang, Y.; Francisco, J. S.; Crawford, T. D.; Bowman, J. M. Dipole Surface and Infrared Intensities for the *cis*- and *trans*-HOCO and DOCO Radicals. *J. Phys. Chem. A* **2013**, *117*, 6932−6939.
(33) See the Supporting Information.
(34) Petty, J. T.; Harrison, J. A.; Moore, C. B. Reactions of *trans*-HOCO Studied by Infrared Spectroscopy. *J. Phys. Chem.* **1993**, *97*, 11194−11198.
(35) Upadhyaya, H. P.; Kumar, A.; Naik, P. D.; Sapre, A. V.; Mittal, J. P. Dynamics of OH Formation in the Dissociation of Acrylic Acid in its (n,π^*) and (π,π^*) Transitions Excited at 248 and 193 nm. *J. Chem. Phys.* **2002**, *117*, 10097.
(36) Zhang, R.-R.; Qin, C.-C.; Long, J.-Y.; Yang, M.-H.; Zhang, B. Ultrafast Predissociation Dynamics of Excited State of Acrylic Acid. *Acta Phys.-Chim. Sin.* **2012**, *28*, 522−527.
(37) Osborne, M. C.; Li, Q.; Smith, I. W. M. Products of the Ultraviolet Photodissociation of Trifluoroacetic Acid and Acrylic Acid. *Phys. Chem. Chem. Phys.* **1999**, *1*, 1447−1454.
(38) Clark, J. M.; Nimlos, M. R.; Robichaud, D. J. Comparison of Unimolecular Decomposition Pathwyas for Carboxylic Acids of Relevance to Biofuel. *J. Phys. Chem. A* **2014**, *118*, 260−274.
(39) Zhao, Y.-L.; Laufer, A. H.; Halpern, J. B.; Fahr, A. Hydrogen Migration and Vinylidene Pathway for Formation of Methane in the 193 nm Photodissociation of Propene: $CH_3CH{=}CH_2$ and $CD_3CD{=}CD_2$. *J. Phys. Chem. A* **2007**, *111*, 8330−8335.
(40) Cingöz, A.; Yost, D. C.; Allison, T. K.; Ruehl, A.; Fermann, M. E.; Hartl, I.; Ye, J. Direct Frequency Comb Spectroscopy in the Extreme Ultraviolet. *Nature* **2012**, *482*, 68−71.